Available online at www.sciencedirect.com
SCIENCE DIRECT®
ELSEVIER
Journal of Hydrology 318 (2006) 374–378
Journal of Hydrology
www.elsevier.com/locate/jhydrol

Utilizing a P-band scatterometer to assess soil water saturation percent of a bare sandy soil

D.G. Blumberg[a,e,*], G. Ronen[b], J. Ben-Asher[c], V. Freilikher[d], L.D. Vulfson[d], A.L. Kotlyar[d]

[a]*Department of Geography and Environmental Development, Ben-Gurion University of the Negev, Be'er Sheva 84105, Israel*
[b]*Department of Environmental and Geological Sciences, Ben-Gurion University of the Negev, Be'er Sheva 84105, Israel*
[c]*The Jacob Blaustein Institute for Desert Research, Ben-Gurion University of the Negev, Sde Boker, Israel*
[d]*Department of Physics, Bar-Ilan University, Ramat Gan 52900, Israel*
[e]*Lamont-Doherty Earth Observatory of Columbia University, New York 10964, USA*

Received 17 May 2004; revised 10 June 2005; accepted 27 June 2005

Abstract

A scatterometer operating in P-band at 441 MHz was used to estimate soil water content. This letter describes encouraging results of experiments that were undertaken in Israel at Yotvata and Ashalim experimental farms. The soil water saturation percent of the entire wetting and drying cycles created through irrigation of sandy agricultural soils were retrieved using the scatterometer, which yielded good agreement with gravimetric measurements of soil water content demonstrating that P-band provides relatively unambiguous estimates of the soil water saturation percent.

Keywords: Radar; Soil water-content; Soil-potential; TDR; P-band; Scatterometer

1. Introduction

Conventional soil moisture measurement techniques (e.g. gravimetric, time-domain reflectometry (TDR), neutron probe, etc.) are generally point-based, and require in situ operators Furthermore, some of them are tedious in post-processing when trying to map the spatial distribution of water content. The scatterometer, on the other hand, can map the spatial variation of larger areas rapidly. The scatterometer uses wavebands similar to many TDRs (441 MHz). The basic principle is that the presence of water in the medium increases the attenuation of the incoming signal and thus, affects the retroreflected signal. In analogy to the TDR, the main premise of the use of a microwave scatterometer for measurements of soil water content comes from the advantages of TDR, which were first introduced by Topp et al. (1980). Generally, the very long wavelength (P-band), makes roughness effects of flat bare soils negligible, unlike shorter wavelength radar systems which are more common (e.g. C and X band systems). Furthermore, the saturation percent is independent of soil texture

* Corresponding author.
E-mail address: blumberg@bgu.ac.il (D.G. Blumberg).

0022-1694/$ - see front matter © 2005 Elsevier Ltd All rights reserved.
doi:10.1016/j.jhydrol.2005.06.023

unlike gravimetric and volumetric measurements. Thus, the expected advantages of using a long wavelength scatterometer to measure the water saturation percent over other expressions of soil water content are twofold (a) acceptable accuracy due to reduced roughness effects, and (b) calibration requirement is limited with respect to soil texture.

In this paper, we shall use a P-band scatterometer to assess changes in the saturation percent (Θ) as a key to estimate soil water content (θ). While most of the existing literature deals with X, C, and L band radar (Ulaby et al., 1996), the use of P-band reduces the effects of roughness significantly and increases the sensitivity to changes in water content following the Fresnel reflection. The depth of penetration is a function of wavelength, and thus at this long wavelength (68 cm) the response will be to the soil water-content at a depth greater than that achieved by the European radar system ERS or other C-band orbiting sensors such as Radarsat. Blumberg et al. (2000) assessed the response as reflecting the water content at a depth of 30% of the wavelength or 15–20 cm using this scatterometer. A detailed theoretical model of the retroreflection from a subsurface in the presence of a dielectric layer such as a high water table is presented in Blumberg et al. (2002). Generally, when the upper soil is saturated the response will be to the water content of the top layer and very little penetration will be achieved. Therefore, in this report we chose to treat the wetting and drying cycles separately with a common transition point at saturation.

Two prime objectives, which can be conceptually placed within the broad topic of precise agriculture and surface hydrology, guided this study:

(a) To use the scatterometer to determine soil water saturation percent from a low altitude that does not require an aircraft (i.e. mounted on a cherry picker).
(b) To monitor the changes in soil–water content of a sandy soil by remote sensing during and following irrigation.

Achieving these objectives would demonstrate the suitability of this technique to measure spatial patterns of soil water-content from an aircraft or as a component of a free flyer satellite program.

2. Materials and methods

The study was conducted at two sites, which are dominated by sandy soils (95–97% sand). The scatterometer is a P-band, 441 MHz continuous wave frequency modulated (CWFM) system meaning that there is a continuous output with two dipoles one of which transmits and one receives energy. The scatterometer field of view is determined by the area of the first Fresnel zone with radius r, which is determined as $r=\sqrt{H\lambda/2}$, where H and λ are the scatterometer altitude above the ground and the wavelength of the radiated signal correspondingly. A further detailed description of the scatterometer, is given by Blumberg et al. (2000) and Daniels et al. (2003a,b).

The wetting cycle was achieved by sprinklers, which supplied water to the soil surface that was observed by the scatterometer. The sprinkling rates ranged from 35 to 44 mm/h. At these rates the soil reached saturation after 3–15 min of wetting followed by up to 48 h of drying. The soil surface samples were collected in the external periphery, outside of the field of view of the scatterometer in order not to disturb the measurements by the scatterometer. During the wetting phase, the samples were collected every 30 s and during the drying phase they were collected at increasing time intervals every 30 s and then at time intervals of up to 10 min apart for 48 h; the samples were collected from 0 to 5 cm depth and treated gravimetrically. The use of a CWFM scatterometer required calibration to some form of absolute values. This was achieved by normalizing the values as shown later in this paper.

3. Results and discussion

Field measurements of gravimetric water content (Fig. 1(A) and (B)) show values ranging from ~1% in the upper 5 cm before irrigation to close to 25% when ponding was evident at the surface.

It is evident from these figures that the wetting phase exhibits a rapid increase in water content after irrigation starts. During the drying phase, the water content decreased from about 22 to 4%.

The corresponding response of the scatterometer is given in Fig. 2(A) and (B). The general trend is similar

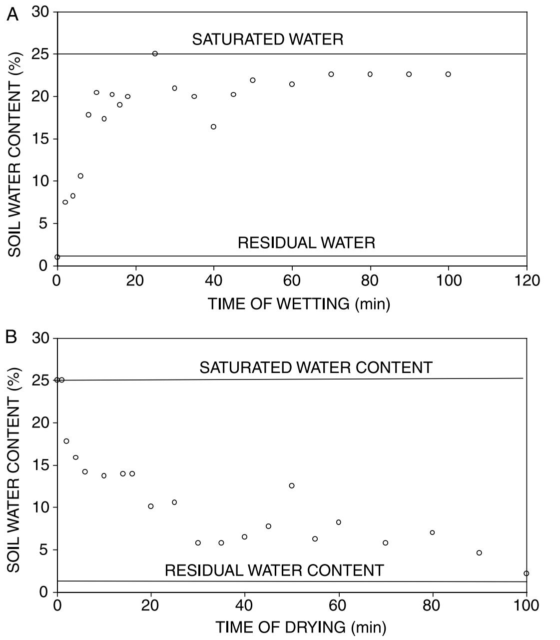

Fig. 1. Typical changes in the gravimetric water content as a function of time during an experiment at Yotvata. The upper and lower lines denote the upper and lower limits of water content: (A) is the wetting phase, whereas (B) is the drying phase.

to the measurements of gravimetric water content shown in Fig. 1. Fig. 2(B) shows that the drying phase extended for 120 min, which is when the drying limb approached its asymptotic value.

The qualitative agreement between the results of the scatterometer and the trends of the water content are encouraging but insufficient for quantitative interpretation of the results. To quantify, the results we assumed that the measured soil water-content (θ) at any time, t, is the weighted average of the saturated pores (θ_s) and the pores with residual water content (θ_r)

$$\theta = \alpha^* \theta_s + (1-\alpha^*)\theta_r \quad (1)$$

where α^* is the fraction of the saturated pores in the soil volume.

From Eq. (1) it is shown that:

$$\alpha^* = (\theta-\theta_r)/(\theta_s-\theta_r) = \Theta \quad (2)$$

Thus, one should note that the right-hand side of Eq. (2) is identical to the dimensionless water content (Θ) of (vanGenuchten, 1980). Hence, α^* which is often marked as Θ is a useful function of the soil hydraulic properties.

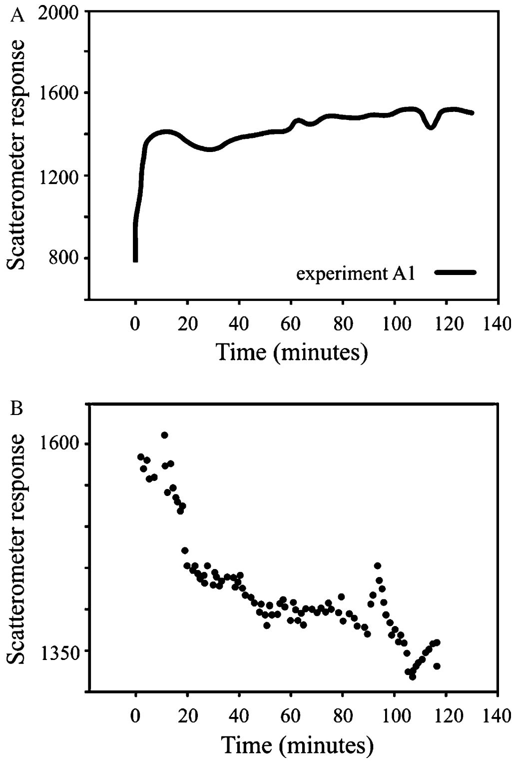

Fig. 2. (A) The scatterometer response during the time of the wetting phase, and (B) the scatterometer response during the drying phase up to 120 min after irrigation was halted and drying started.

The saturation percent is a most valuable variable to evaluate the soil water potential and the retention curve 'θ–h' using Eq. (3)

$$\Theta = \frac{\theta-\theta_r}{\theta_s-\theta_r} = [1+|\alpha h|^n]^{(1-n)/n} \quad (3)$$

where θ_r, θ_s, θ, and Θ were previously determined, α^* is a positive scaling factor for length (units L^{-1}) and h is the pressure head (units L) where $n \sim 1.5$.

The two other important variables that can be derived from the scatterometer are the unsaturated hydraulic conductivity function (of vanGenuchten, 1980, for example) and the straight forward actual water content, assuming θ_r is the water retained at $h=$ 1.5 MPa and θ_s is the measured saturation water content or alternatively pore volume. Thus, actual water content θ can also be evaluated from the results.

From Fig. 1(A), we can observe that Θ is the fraction of the saturated pores at any given time during the wetting process. It changes rapidly when the dry fraction $(1-\Theta)$ is large, and slowly when $(1-\Theta)$ is small. Therefore, we assume that $\mathrm{d}\Theta/\mathrm{d}t$ is a linear function of $(1-\Theta)$ with a negative slope 'k' which is a combined characteristic of irrigation intensity and soil hydraulic properties (t^{-1}), such that:

$$\frac{\mathrm{d}\Theta}{\mathrm{d}t} = -k(1-\Theta) \tag{4}$$

After reorganization and integration Eq. (4) yields:

For the wetting phase : $\Theta = 1-\exp(-kt)$ (5a)

and

For the drying phase $\Theta = \exp(k^{*}(t-T_{\mathrm{w}}))$ (5b)

We define T_{w} as the time to start the drying process such that when sprinkling stops $t-T_{\mathrm{w}}=0$.

The schematic of the two phases is shown in Fig. 3 and the actual processes are shown in Fig. 4, which includes all experimental runs. Fig. 3 presents a practical method to estimate the values of k and k^* from the field measurements. Fig. 4 shows the behavior of Θ that was normalized from gravimetric θ measurements (circles) and from the scatterometer (triangles). These reached their maximum values together and the drying process started when $\Theta=1$. Therefore, the two forms of Eq. (4) are continuous and have the same value of Θ at $t=T_{\mathrm{w}}$. A regression analysis in which we assessed the scatterometer values of Fig. 4 as a function of the measured Θ yielded a slope close to unity (0.95) and a $r^2=0.8$. This indicates that the scatterometer successfully identified the actual saturation percent that was determined from gravimetric measurements.

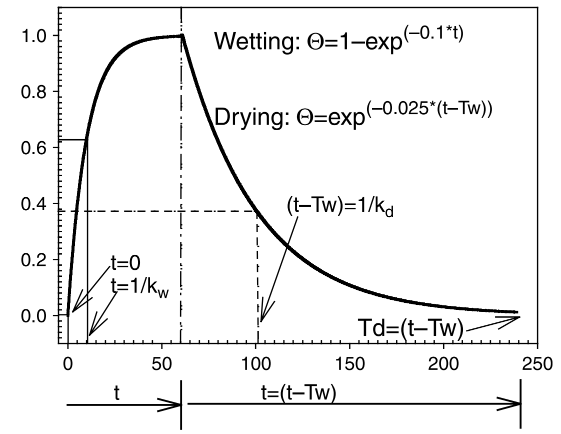

Fig. 3. (A) schematic of the model behavior described in Eqs. (4). The irrigation intensity constant, k_{w}, is determined by the time when $(1-\Theta)=1/e$ of its maximal value, (i.e. when the soil saturation is approximately 2/3 of its maximum) and is marked by the solid line. The drying constant, k^*, is obtained at $\Theta=1/e$ or approximately 1/3 of its maximal value. The wetting and drying phases are separated by the vertical dashed line. The horizontal dashed line marks the time from which k^* is determined.

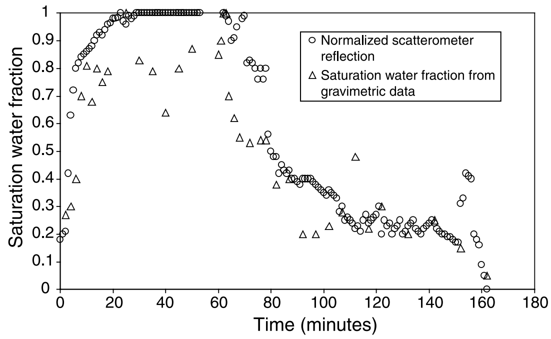

Fig. 4. Summary of all experiments combining wetting and drying processes. The gravimetrically measured water saturation fraction (triangles) and the corresponding normalized scatterometer response (circles) are presented as a function of time from the beginning of the wetting phase until the end of the drying phase.

4. Concluding remarks

The low frequency (441 MHz) and the long wavelength (68 cm) scatterometer can provide a first approximation of Θ. It has an advantage over previous work that utilized L-band radar data in that most agricultural soils will be smooth relative to the wavelength of the scatterometer. Moreover, at these long wavelengths the scatterometer can observe through small vegetation although the amplitude change caused by the vegetation would need to be modeled in future work. At this stage the scatterometer can be used only to determine soil water saturation percent and to monitor its changes along continuous time intervals. However, improving the formulation of a theoretical model to describe more rigorously the relationship between saturation percent, dielectric constant, and the reflection coefficient may generalize the results to other soil textures and then to measuring spatial patterns of soil water-content. So far there are no free flying SAR systems at P-band because of the large antenna requirements at this wavelength. However, this application amplifies the need for such an instrument on future Earth Observing missions.

Acknowledgements

The authors wish to acknowledge the funding agencies for funds made available to this work. These include a strategic infrastructure grant provided by the Israel Space Agency (ISA), a grant provided by the United States Office of Naval Research (ONR), and by a grant from Ministry of Science Israel and the Bundesministerium fuer Bildung und Forschung (BMBF). The work could not be achieved without the collaboration of those working the Ashalaim and Yotvata experimental farms. Roni Blaustein Livnon is acknowledged for her help with some of the figures. Part of the senior author's (DGB) work was done while at the Lamont Doherty-Earth Observatory at Columbia University.

References

Blumberg, D.G., Freilikher, V., Lyalko, I.V., Vulfson, L.D., Kotlyar, A.L., Shevchenko, V.N., Ryabokonenko, A.D., 2000. Soil moisture (water-content) assessment by an airborne scatterometer: the Chernobyl disaster area and the Negev desert. Remote Sensing of Environment 71 (3), 309–319.

Blumberg, D.G., Freilikher, V., Fuks, I., Kaganovskii, Y., Maradudin, Aa, Rosenbluh, M, 2002. Effects of roughness on the retroreflection from dielectric layers. Waves in Random Media 12 (3), 279–292.

Daniels, J., Blumberg, D.G., Vulfson, L.D., Kotlyar, A.L., Freiliker, V., Ronen, G., Ben-Asher, J., 2003. Microwave remote sensing of physically buried objects in the Negev Desert: implications for environmental research. Remote Sensing of Environment 86 (2), 243–256.

Daniels, J., Blumberg, D.G., Vulfson, L.D., Kotlyar, A.L., Freiliker, V., Ronen, G., Ben-Asher, J., 2003b. Microwave remote sensing of physically buried objects in the Negev desert: Implications for subsurface Martian exploration. Journal of Geophysical Research-Planets 108 (E4).

Topp, G.C., Davis, J.L., Annan, A.P., 1980. Electromagnetic determination Of soil-water content-measurements in coaxial transmission-lines. Water Resources Research 16 (3), 574–582.

Ulaby, F.T., Dubois, P.C., vanZyl, J., 1996. Radar mapping of surface soil moisture. Journal of Hydrology 184 (1-2), 57–84.

vanGenuchten, A., 1980. Closed-Form Equation for Predicting the Hydraulic Conductivity of Unsaturated Soils. Soil Science Society of American Journal 44, 892–898.